TESS light curves analysis for 24 hot Jupiters

Qiyu Li[1],[†], Rachel H. Yang[2],[6],[†], Wenrui Zhang[3],[†], Yuyan Zou[4],[†], Junzhe Shi[5],[†]

[1]University of Science and Technology of China, Hefei, 230026, China
[2]Burr & Burton Academy, Manchester, Vermont, 05254, U.S
[3]Merchiston International School, Shenzhen, 518000, China
[4]Basis International School, Huizhou, 516200, China
[5]Wuhan Britain-China School, Wuhan, 430010, China

[6]ryang25@burrburton.org
[†]These authors contributed equally to this work and should be considered co-first authors.

Abstract. The precise planet ephemeris can provide useful reference for future investigations and observations. With the continuous data returned by NASA Transiting Exoplanet Survey Satellite (TESS), we are able to continuously refine the planet's transits. We analyzed the data sent back from TESS as well as other previous data using Mandel & Agol model and Markov Chain Monte Carlo (MCMC) ensemble sampler to obtain the best-fit planetary parameters of 24 hot Jupiters. Our data leads to a detection of orbital-decay for HATS-1b and WASP-19b and each has a decreasing rate of $dP/dt = -22.77 \pm 7.49\ ms\ yr^{-1}$ and $dP/dt = -2.95 \pm 0.51\ ms\ yr^{-1}$. HATS-1, was detected for the first time to have an orbital decay trend. When analyzing data plots, we came across some special features in light curves, such as periodic smaller dips in the system of WASP-24, leading to the detection of a possible new planet. We hope our findings will provide helpful references for future studies and observations.

Keywords: hot Jupiters, orbital decay, exoplanets.

1. Introduction

People have long been curious about the planets outside our solar system. Hot Jupiters happen to be one of the most mysterious ones among them. They have large masses (0.36-11.8 M_{Jup}), but at the same time, short orbital periods (P < 10 days) with low eccentricities [1]. Through long-term observation, we have the possibility to detect some astrophysical phenomena, such as tidal orbital decay [2,3]; apsidal precession [4]; gravitational interference by nearby masses [5,6] and etc. However, these phenomena are rare in the case of hot Jupiter [7].

Transiting Exoplanet Survey Satellite (TESS [8]), the most recent major exoplanet discovery mission, aims to find exoplanets through the transit method [9]. As of 4/13/2023, TESS had detected a total of 6400 candidate signals and confirmed 329 planets. Public data releases every 4 months, encouraging rapid community-wide efforts to investigate the new planets. Every round of new data enables us to make our estimates on the planets' ephemerides more accurate. Taking this opportunity, we have analyzed the light curves and refined the parameters for 24 hot Jupiters using the newest data sent back

from TESS along with the previous data. The planets are selected by having both past data and 2023 data (excluding WASP-24).

The parameters include the planet's orbital period P, the time of conjunction T_c, the orbit-to-star radius ratio $a/R\star$, the impact parameter b, the planet-to-star radius ratio $Rp/R\star$, and one limb-darkening coefficient u. These parameters, particularly transit timings, can provide very useful evidence for orbital changes. We have also selected ones with abnormal features requiring further analysis. We hope our work will provide helpful references for future investigations.

The paper is organized as follows. Section 2 describes the methods and models we used. Section 3 summarizes and analyzes our results. Section 4 concludes the sections above and gives further discussion.

2. Light Curve Modeling

We wrote two half-automatic codes to download and process data from TESS taking reference from Ivshina & Winn [10]. The first one uses routines from the lightkurve Python package to download any available light curves, then fitted the model, for which to get all the parameters and their uncertainties [11,12]. But the $a/R\star$, b, $Rp/R\star$, u uncertainties obtained through this method is particularly high, so we wrote a second code. The second one is employed with a Markov Chain Monte Carlo method (MCMC; [13]) to only process the latest sector data of TESS to get the estimates for the parameters mentioned and their uncertainties. Below we have a brief explanation of how we did it.

2.1. Time of Conjunction and Period

Flux vs time is obtained from the data of TESS, and the nearest neighbors of each transit are extracted based on the previous Tc and period. The part without transits is flattened to 1 to facilitate subsequent fitting. We then fitted and flatten the data near transit times with a polynomial of 4th degree or less in order to obtain the transit data that is not affected by environmental brightness of the star, which are usually the variations in the star's luminosity and systematic errors. First, the angle of the planet to the z-axis φ is represented by the formula below, where t is the independent variable, t_c stands for time of conjunction and period stands for the period of the planet.

$$\varphi = (2\pi \times (t - t_c))/period \qquad (1)$$

We then calculated the distance of the planet on the x, y, and z axes by angular φ. Where a stands for orbit-to-star radius ratio and b stands for impact parameter.

$$x = asin(\varphi) \qquad (2)$$
$$y = bcos(\varphi) \qquad (3)$$
$$z = \sqrt{a^2 + b^2} \times cos(\varphi) \qquad (4)$$

Finally we used x and y to calculate the distance between the planet and the star on the xy plane and name it sep. If an eclipse occurs the distance should be at its local minimum.

$$sep = \sqrt{a^2 + y^2} \qquad (5)$$

In order to minimize errors, we decided to take the limb darkening effect into account as a proxy for the uneven distribution of luminosity on the planetary surface. Equation (5) will be calculated through the linear limb-darkening model from where $\mu = \sqrt{1 - X^2 - Y^2}$ and u stands for the limb-darkening coefficient [14].

$$\frac{I(\mu)}{I(1)} = 1 - u(1 - \mu) \qquad (6)$$

In order to obtain more precise parameters, we define tlc_residuals to output the quantified the difference between theoretical and observed values named res. The quantized values will be minimized with lmfit in order to obtain the minimum value of X^2, which is the square of res. This method is derived from Levenberg-Marquardt and is a least squares estimation. We chose the chi-square method due to its description of the average deviation of the observed and theoretical values, and also convenient to write acceptance probabilities when applying MCMC (Markov Chain Monte Carlo) at a later time.

Subsequently, in order to get a more precise estimate on t_c and period, they will be used as a single parameter to do linearization for each transit. In the equation below, m represents period, b indicated the time zero which is the t_c of the 0th transit, and the choice is arbitrary. Through this step, we got our final value for t_c and period. For this step, we used all the TESS sectors and the previous data from other telescopes.

$$t_c = m \times (orbit\ number) + b \tag{7}$$

By fixing these two parameters, we obtained the distribution of the other parameters.

2.2. Other Parameters

We realized that our uncertainties in parameters a, b, k, u was far higher than data in previous literature, so we employed a Markov Chain Monte Carlo method to quantify parameter uncertainties. This overall model is a composition of a polyfit function and a transit model. The ployfit function is usually a polynomial of some degree that is used to model stellar brightness and time, which is typically influenced by stellar speckles, stellar activity, or instrumental noise. We constructed likelihood functions to assess the probability of obtaining light-curve data using the chi square model, conditional on the combined model parameters (the coefficients of the multi-fit function and the Lingzhi model parameters). Polyfit function is combined with the transit model to generate a synthetic light curve for each parameter set in the chain. Then we compare the synthetic light curve to the observed data and the likelihood function is evaluated. It's worth noting that a priori distributions were introduced for all model parameters, including the polyfit function coefficients and the transit model parameters. The MCMC algorithm generates a series of parameter sets (chains) in the combined parameter space. At each iteration, it proposes a new set of parameters and computes the likelihood of the data given those parameters and a priori probabilities. The Metropolis-Hastings algorithm is a commonly used algorithm in MCMC. We used this method and started with the parameters from lmfit in each sector as initial values, performed a total of 400,000*5 sampling iterations, with each iteration consisting of 100,000 warm-up steps.

3. Results & Analysis

Applying the model discussed in section 2 to the TESS data of 24 hot Jupiters, we obtained our estimates on the parameters provided in Table 1, where P is the orbital period of the planet and t_c is the time conjunction (transit mid-point). The rest of the parameters including the ratio of planet radius to stellar radius R_p/R_*, the ratio of semi-major axis to stellar radius a/R_*, the transit impact parameter b, and the limb darkening coefficient u are included in Table 2. We used light curves generated by Science Processing Operations Center SPOC ("source") having a 120s time sampling ("cadence").

Table 1. Collection of fitted P(days) and T_c.

Source	Cadence
SPOC	120

Planet	P(days)	T_c
HAT-P-30b	2.810505496± 5.29e-7	2459987.155398 ± 2.81e-4
HAT-P-35b	3.646658878 ± 6.85e-7	2459987.471459 ± 4.36e-4
HAT-P-42b	4.641839020 ± 9.10e-7	2459986.284833 ± 2.94e-4
HAT-P-43b	3.332680600 ± 4.55e-7	2459986.590582 ± 3.40e-4
HAT-P-69b	4.78695540 ± 2.87e-6	2459984.536857 ± 6.05e-4
HATS-1b	3.446454790 ± 5.18e-7	2460038.7541445± 1.99e-4
HATS-2b	1.354133510± 3.92e-7	2460038.653460± 2.76e-4
HATS-42b	4.641839020 ± 9.10e-7	2459986.284833 ± 2.94e-4

Table 1. (continued)

HATS-52b	1.366655842 ±1.80e-7	2460013.573148 ± 2.15e-4
HATS-53 b	3.853777657 ± 7.03e-7	2460038.453452 ± 3.09e-4
HATS-54 b	2.54417317 ± 1.59e-6	2460067.22371 ± 1.19e-3
HATS-55 b	4.20418904 ± 2.12e-6	2459986.09454 ± 1.09e-3
HATS-56 b	4.32476565 ± 2.52e-6	2460062.830483 ± 5.70e-4
HATS-58 A b	4.21807417 ± 2.27e-6	2460065.852239 ± 4.77e-4
HATS-7b	3.1853146±1.46e-5	2460063.9972±1.52e-2
WASP-119 b	2.499804310 ± 2.43e-7	2460149.76686 ± 1.30-4
WASP-121b	1.2749250000 ± 7.55e-8	2459987.4855400 ± 7.00e-5
WASP-132b	7.133513434 ± 9.40e-07	2460086.626770 ± 1.95-04
WASP-142b	2.05286718 ± 1.24e-6	2460013.180560 ± 4.58e-4
WASP-170b	2.344778090 ± 2.88e-7	2460013.517820 ± 1.68e-4
WASP-19b	0.7888388160 ± 8.60e-8	2460040.049270 ± 1.01e-4
WASP-23b	2.977642840 ± 8.15e-7	2459253.878931 ± 1.09e-4
WASP-24b	2.341220330 ± 4.84e-7	2459716.996250 ± 8.92e-4
WASP-65 b	2.3114204400 ± 7.58e-8	2459986.940110 ± 8.04e-5

Table 2. Collection of the rest of the fitted parameters.

Planet	Sector	a/R_*	b	R_p/R_*	u
HAT-P-30b	61	6.73±0.28	0.86±0.03	0.108±0.002	0.31±0.26
HAT-P-35b	61	7.10±0.38	0.38±0.15	0.090±0.002	0.25±0.13
HAT-P-42b	61	5.73±0.25	0.24±0.14	0.094±0.002	0.21±0.16
HAT-P-43b	61	8.25±0.44	0.31±0.16	0.118±0.003	0.18±0.12
HAT-P-69b	48	7.69±0.23	0.20±0.13	0.0850±0.0006	0.30±0.06
HATS-1b	63	9.72±0.34	0.68±0.03	0.126±0.001	0.46±0.10
HATS-2b	63	5.69±0.14	0.19±0.11	0.13±0.001	0.44±0.06
HATS-7b	64	7.21±1.38	0.75±0.18	0.074±0.004	0.38±0.26
HATS-42b	64	8.82±3.15	0.49±0.28	0.000005±0.000033	0.49±0.28
HATS-52b	62	5.56±0.17	0.24±0.13	0.142±0.002	0.20±0.11
HATS-53b	63	8.91±0.54	0.38±0.16	0.129±0.002	0.31±0.13
HATS-54b	64	8.07±1.50	0.45±0.27	0.077±0.008	0.67±0.24
HATS-55b	61	12.73±1.31	0.44±0.20	0.133±0.004	0.30±0.20
HATS-56b	64	6.54±0.62	0.60±0.13	0.080±0.002	0.42±0.11
HATS-58 A b	64	6.95±0.55	0.81±0.05	0.091±0.002	0.51±0.22
WASP-19b	63	3.58±0.05	0.64±0.02	0.1473±0.0009	0.54±0.05
WASP-23b	61	19.30±5.94	0.50±0.29	0.00001±0.00010	0.50±0.28
WASP-24b	51	5.77±0.33	0.68±0.05	0.1029±0.0008	0.16±0.10
WASP-65	61	6.65±0.26	0.40±0.11	0.117±0.001	0.39±0.05
WASP-119	67	7.14±0.25	0.27±0.13	0.11±0.001	0.41±0.05

Table 2. (continued)

WASP-121b	61	3.71±0.04	0.23±0.06	0.1220±0.0006	0.20±0.05
WASP-132b	65	18.89±0.95	0.22±0.16	0.125±0.002	0.42±0.08
WASP-142b	62	4.18±0.18	0.81±0.02	0.102±0.002	0.19±0.13

3.1. Long-term Transit Variations

To spot evidence for orbital decay, we fitted a model from [2] to all of the previous transits assuming the orbit is circular and the orbital period is changing uniformly with time, where N is the number of orbits and T_0 is the mid transit time,

$$t_{tra}(N) = T_0 + NP + \frac{1}{2}\frac{dP}{dN}N^2 \tag{8}$$

the implied period derivative is shown by,

$$\frac{dP}{dt} = \frac{1}{P}\frac{dP}{dN} \tag{9}$$

We paid special attention to those for which dP/dN was found to be bigger than 3σ from zero:

3.2. HATS-1 b

HATS-1 b is a planet orbiting a G-type main sequence star. HATS-1 b has a period of P ≈ 3.4465 days, mass of Mp ≈ 1.86 Mj, and radius of Rp ≈ 1.30 Rj [15,16]. The host star has a mass of 0.99 M⊙ and radius of 1.04 R⊙, which is very similar to our sun [15]. Up to our knowledge, no literature has been found to prove the decaying trend of HATS-1 b. The timing residuals are shown in Figure 1. The best-fit model has dP/dt = -22.77±7.49 ms yr-1.
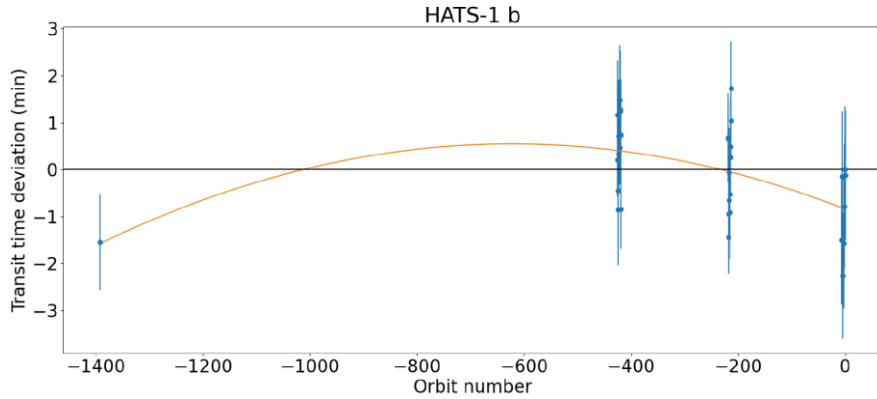

Figure 1. Timing residuals of HATS-1 b. Transit times are shown in blue. The best-fit model curve is shown in orange. P=3.446454790 ± 0.000000518 T_c=2460038.7541445± 0.000199.

3.3. WASP-19 b

WASP-19 b is a planet which has a period of P ≈ 0.7888 days, mass of Mp ≈ 1.15 Mj, and a radius of Rp ≈ 1.42 Rj [17,18], orbiting a G8V star [19]. Due to its short period of less than a day, it has always been considered one of the most favorable planets to search for orbital decay. Ivshina & Winn [17] found that dP/ dt = −3.54 ± 1.18 ms yr-1. Our best-fit model shows that dP/dt = -2.95±0.51 ms yr-1. The timing residuals are shown in Figure 2.

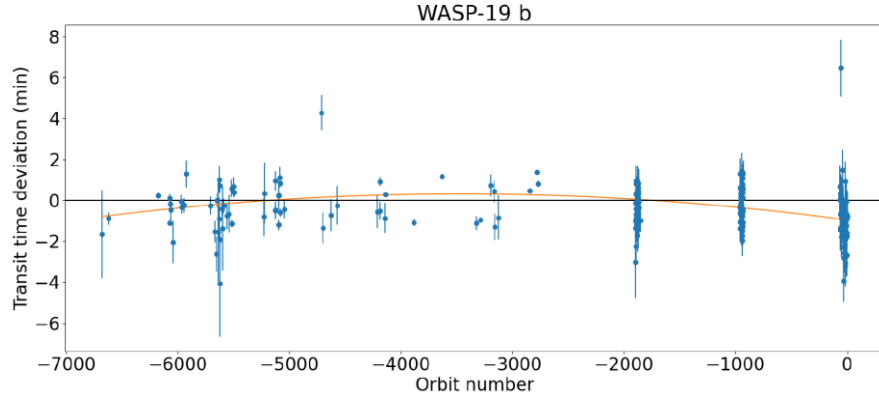**Figure 2.** Timing residuals of WASP-19 b. Transit times are shown in blue. The best-fit model curve is shown in orange. P=0.7888388160±0.000000086 T_c=2460040.049270±0.000101.

Table 3. Decay rates for HATS-1b, WASP-19b.

Planet	dP/dN (days)	dP/dt (ms yr^{-1})
HATS-1b	$(-4.97 \pm 1.64) \times 10^{-9}$	-22.77 ± 7.49
WASP-19b	$(-14.75 \pm 2.54) \times 10^{-11}$	-2.95 ± 0.51

The search for evidence of orbital decay requires long-term observations. The projected rate of orbital decay is just offered as an indication due to the insufficiency of orbital and transit data for the planets. We intend to keep updating this data in the future when more data is released while inviting any interested researchers to continue doing the same (see Table 3).

3.4. Features in Light Curves
While looking at the light curves of each planet, we discovered some unexpected features in the following systems:

4. WASP-24
WASP-24 shows periodic dips besides those due to WASP-24 b throughout the entire light curve. See Figure 3. We couldn't see another star or a binary system that was causing the dips by looking at the pixel file of the sky region around WASP-24. An exciting possibility is that we've detected a small inner transiting planet. However, we still need more data to support this idea, since this is the only available sector of TESS data so far. We hope TESS can revisit this system to help obtain more evidence for this new planet.
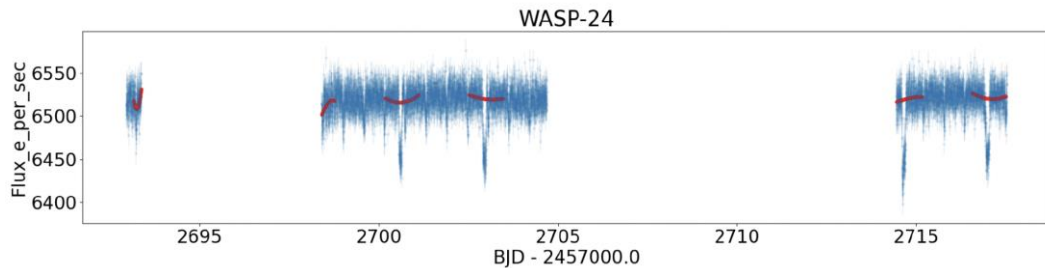

Figure 3. WASP-24 sector 51 light curve.

5. WASP-23

In the system of WASP-23, we observed periodic rises in the light curves of sector 34 (2021) and 61 (2023), but not in sector 6 (2018), shown in Figure 4. After checking the pixel file, we found that the period of the rises highly matches the period of a star's eclipse on the up right of WASP-23. Our guess is that it's a binary of two main sequence stars. We can infer that one of the stars is hotter and more luminous than the other, since one of the eclipses is much deeper than the other one. See Figure 5. Due to the fact that this binary system is relatively closer to us, when we observed eclipses, the star was actually during its occultations on the opposite side, resulting in this opposite light curve. As for why there was no such phenomenon in 2016, we speculate that it was due to a change in the position of the star.
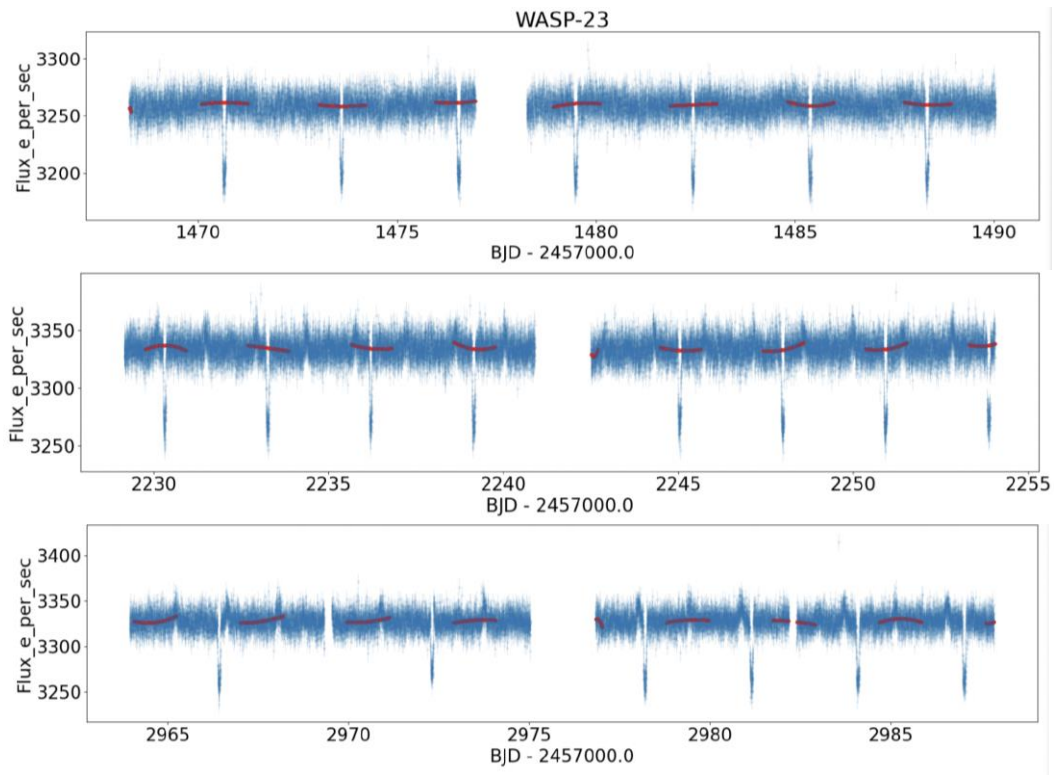

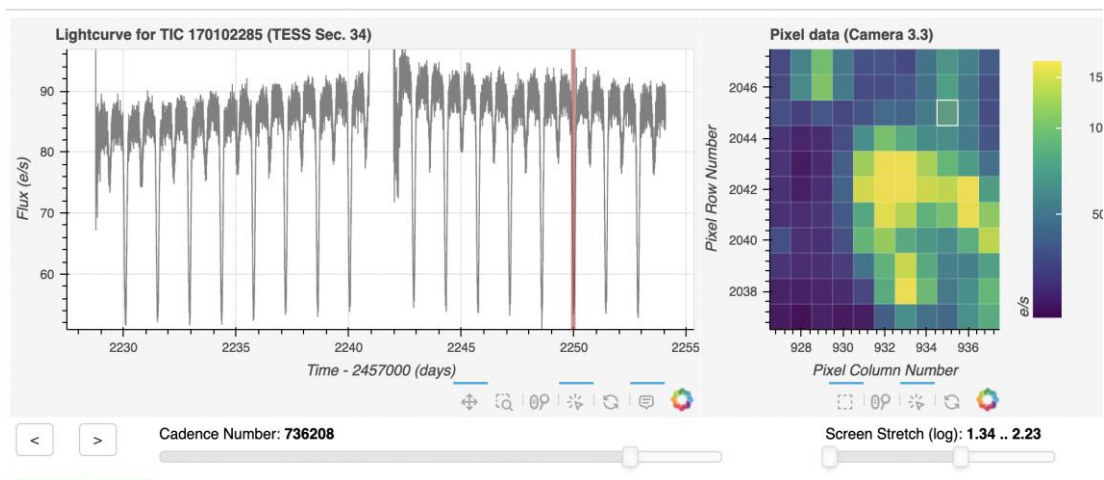**Figure 4.** WASP-23 sector 6, sector 34 and sector 61 light curves.

Figure 5. Light curve for a star on the up right of WASP-23.

6. WASP-28

WASP-28 shows a brightening event at around TESS JD 2470 (sector 42). We went to look at the pixel file of WASP-28 and noticed that there is an unknown glowing object passing in front of WASP-28 in a short period of time. This object has a brightness of the brightness that was occultated by the planet. So far, the inference about this object is that it is an asteroid.

7. HATS-54

HATS-54 shows two brightening events at around TESS JD 2314 (sector 37) and 3045 (sector 64). Apparently, these events are unrelated to the system HATS-54. We checked the TESS images and clearly saw a glowing object passing through the sky region during the second brightening event.

8. WASP-132

WASP-132 shows a brightening event near TESS JD 3090 (sector 65). Inspection of the images showed that the brightening event was caused by an enormous glowing object (almost the size of the host star) passing quickly in front of WASP-132. But this rapidly passing glowing object is likely to be just an asteroid that is relatively closer to us, making it look just as big as the star.

9. Conclusion

Through analyzing TESS data, we improved the precision of period and time conjunction of 24 hot Jupiters, and also gave our own estimates on the parameters including a, b, k, u. We hope our database can provide useful information for those who are interested in investigating them in the future, such as those who are seeking long-term transit variations. We also discovered and provided evidence to some planets that may are orbital decaying including WASP-19 b and HATS-1 b, which have decay rates of dP/dt=-2.95±0.51 ms/yr and dP/dt = -22.77±7.49 ms/yr. However, our estimated decay rate of WASP-19 b seems to be contradicting the statement that any period changes of WASP-19 b are slower than 2.2 ms/yr by Petrucci et al. [20]. HATS-1, was discovered for the first time to have an orbital decay trend. We encourage astronomers as well as TESS to keep paying attention to these systems, especially HATS-1, to provide stronger evidence for orbital decay. During the process, we also detected a new planet in the system of WASP-24, although we still need more evidence to verify our conjecture. Long-term transit timing monitoring is essential to discover orbital decay. Therefore, we will continue to monitor the transit times of hot Jupiters and encourage all astronomy enthusiasts to make good use of TESS's public data to update the data together.

Acknowledgement

References
[1] Fabrycky, Daniel, and Scott Tremaine. "Shrinking binary and planetary orbits by Kozai cycles with tidal friction." The Astrophysical Journal, vol. 669, no. 2, 2007, pp. 1298–1315, https://doi.org/10.1086/521702.
[2] Patra, Kishore C., et al. "The continuing search for evidence of tidal orbital decay of Hot Jupiters." The Astronomical Journal, vol. 159, no. 4, 2020, p. 150, https://doi.org/10.3847/1538-3881/ab7374.
[3] Yee, Samuel W., et al. "The orbit of WASP-12B is decaying." The Astrophysical Journal, vol. 888, no. 1, 2019, https://doi.org/10.3847/2041-8213/ab5c16.
[4] Ragozzine, Darin, and Aaron S. Wolf. "Probing the interiors of very hot Jupiters using transit light curves." The Astrophysical Journal, vol. 698, no. 2, 2009, pp. 1778–1794, https://doi.org/10.1088/0004-637x/698/2/1778.
[5] Miralda-Escude, Jordi. "Orbital perturbations of transiting planets: A possible method to measure stellar quadrupoles and to detect earth-mass planets." The Astrophysical Journal, vol. 564, no. 2, 2002, pp. 1019–1023, https://doi.org/10.1086/324279.

[6]   Holman, Matthew J., and Norman W. Murray. "The use of transit timing to detect terrestrial-mass extrasolar planets." Science, vol. 307, no. 5713, 2005, pp. 1288–1291, https://doi.org/10.1126/science.1107822.

[7]   Steffen, Jason H., et al. "Kepler constraints on planets near Hot Jupiters." Proceedings of the National Academy of Sciences, vol. 109, no. 21, 2012, pp. 7982–7987, https://doi.org/10.1073/pnas.1120970109.

[8]   Ricker, George R., et al. "Transiting Exoplanet Survey Satellite." Journal of Astronomical Telescopes, Instruments, and Systems, vol. 1, no. 1, 2014, p. 014003, https://doi.org/10.1117/1.jatis.1.1.014003.

[9]   Winn, Joshua N. "Transits and Occultations." arXiv e-prints, 2014, https://doi.org/10.48550/arXiv.1001.2010.

[10]   Ekaterina S. Ivshina, & Joshua N. Winn. (2022). transit-timing/tt: Transit Timing En Masse (Version v0). Zenodo. https://doi.org/10.5281/zenodo.5904270.

[11]   Lightkurve Collaboration. "Lightkurve: Kepler and TESS time series analysis in Python" Astrophysics Source Code Library, 2018, record ascl:1812.013. http://ascl.net/1812.013.

[12]   Mandel, Kaisey, and Eric Agol. "Analytic light curves for planetary transit searches." The Astrophysical Journal, vol. 580, no. 2, 2002, https://doi.org/10.1086/345520.

[13]   Czesla. "PyA: Python astronomy-related packages." Astrophysics Source Code Library, record ascl:1906.010, 2019, https://ui.adsabs.harvard.edu/abs/2019ascl.soft06010C.

[14]   Claret, A. "Limb and gravity-darkening coefficients for the Tess satellite at several metallicities, surface gravities, and microturbulent velocities." Astronomy & Astrophysics, vol. 600, 2017, https://doi.org/10.1051/0004-6361/201629705.

[15]   Penev, K., et al. "Hats-1B: The first transiting planet discovered by the HATSouth survey." The Astronomical Journal, vol. 145, no. 1, 2012, p. 5, https://doi.org/10.1088/0004-6256/145/1/5.

[16]   Bonomo, A. S., et al. "The GAPS programme with HARPS-N at TNG." Astronomy & Astrophysics, vol. 602, 2017, https://doi.org/10.1051/0004-6361/201629882.

[17]   Ivshina, Ekaterina S., and Joshua N. Winn. "Tess Transit timing of hundreds of hot Jupiters." The Astrophysical Journal Supplement Series, vol. 259, no. 2, 2022, p. 62, https://doi.org/10.3847/1538-4365/ac545b.

[18]   Cortés-Zuleta, Pía, et al. "Tramos." Astronomy & Astrophysics, vol. 636, 2020, https://doi.org/10.1051/0004-6361/201936279.

[19]   Hebb, L., et al. "WASP-19B: The shortest period transiting exoplanet yet discovered." The Astrophysical Journal, vol. 708, no. 1, 2009, pp. 224–231, https://doi.org/10.1088/0004-637x/708/1/224.

[20]   Petrucci, R, et al. "Discarding orbital decay in wasp-19b after one decade of transit observations★†." Monthly Notices of the Royal Astronomical Society, 2019, https://doi.org/10.1093/mnras/stz3034.

[21]   Van der Walt, Stéfan, et al. "The NumPy array: A structure for efficient numerical computation." Computing in Science & Engineering, vol. 13, no. 2, 2011, pp. 22–30, https://doi.org/10.1109/mcse.2011.37.

[22]   Hunter, John D. "Matplotlib: A 2D graphics environment." Computing in Science & Engineering, vol. 9, no. 3, 2007, pp. 90–95, https://doi.org/10.1109/mcse.2007.55.

[23]   "Proceedings of the 9th Python in Science Conference." Proceedings of the Python in Science Conference, 2010, https://doi.org/10.25080/majora-92bf1922-012.

[24]   Jones, Eric, Travis Oliphant, and Pearu Peterson. "SciPy: Open source scientific tools for Python.", 2001, https://scipy.org/.

[25]   Newville, Matthew, et al. "Lmfit: Non-Linear Least-Square Minimization and Curve-Fitting for Python." Astrophysics Source Code Library, record ascl:1606.014, 2016, https://ui.adsabs.harvard.edu/abs/2016ascl.soft06014N/abstract.